From Giant Planets to Cool Stars
ASP Conference Series, Vol. 3 × 10⁹, 1999
Caitlin Griffith and Mark Marley, eds.

Condensates in Jovian Atmospheres

Robert A. West
Jet Propulsion Laboratory, California Institute of Technology, 4800 Oak Grove Drive, Pasadena, CA 91109

Abstract. Thermochemical equilibrium theory which starts with temperature/pressure profiles, compositional information and thermodynamic data for condensable species in the jovian planet atmospheres predicts layers of condensate clouds in the upper troposphere. The deepest of these is a water/ammonia solution near the 6-bar pressure level for Jupiter. At higher altitudes H_2S and NH_3 react to form NH_4SH which is predicted to condense in Jupiter's atmosphere near 2 bars pressure. At higher levels NH_3 or H_2S will condense, depending on which of these is depleted first during formation of the NH_4SH cloud. Observations indicate that ammonia forms the upper cloud in the atmospheres of Jupiter and Saturn while hydrogen sulfide forms this cloud in the atmospheres of Uranus and Neptune. Methane ice clouds are present at higher altitudes in the atmospheres of Uranus and Neptune. An abundance of remote and (for Jupiter) *in situ* observations provide information on particle optical depths and sizes, at least for the uppermost cloud layer. In spite of all this information good microphysical models for cloud particle size distribution and optical depth remain elusive because they require detailed knowledge of atmospheric dynamics and cloud microphysics much beyond what is now possible.

1. Introduction

Condensate particles and gas molecules in the atmospheres of the jovian planets (Jupiter, Saturn, Uranus and Neptune) control the intensity of sunlight reflected from the atmosphere and the spectral content of radiation emitted by the atmosphere. They are also play a fundamental role in the temperature structure and energy budget of the atmosphere. Knowledge of the chemistry and physics of clouds in the giant planets observed close at hand is therefore valuable to guide the interpretation of observed spectra of extrasolar planets when they become available and to construct models of the atmospheres of those objects. This contribution summarizes theoretical models and analyses of observations pertaining to condensate clouds in the jovian atmospheres.

2. Thermochemical Equilibrium and Cloud Microphysics Theory

Armed with knowledge of the temperature/pressure profile and abundances and thermodynamic properties of molecules in the deep atmosphere (where the tem-

Figure 1. Temperature/pressure profiles for the jovian planets and condensation vapor pressure curves for methane, ammonia and water (from Gierasch Conrath, 1993). The solid parts of the curves are based on temperatures retrieved from Voyager data. The dashed parts are adiabatic extrapolation to deeper levels. Condensate clouds form where indicated.

peratures are too high for condensation and condensable molecules are well mixed), atmospheric chemists have constructed models of condensation regions governed by the laws of thermochemical equilibrium theory. Fig. 1 (Gierasch & Conrath, 1993) shows pressure/temperature profiles for the four jovian planets and illustrates where the vapor pressure curves for CH_4, NH_3 and H_2O cross these, defining the base of the cloud layer.

Current cloud condensation models are rooted in the work of Lewis (1969) and Weidenschilling & Lewis (1973). These models remain essentially intact today, although recent improvements in our understanding of pressure/temperature profiles and abundances of condensable species have led to improved models. Figure 2 shows a more recent incarnation of these models. The cloud densities plotted in Fig. 2 are meant to be illustrative rather than definitive. They were calculated for an idealized model where the amount of condensate at some pressure level is given by the amount available to condense for vapor slowly diffusing upward. Atmospheric dynamics and microphysical processes will greatly modify this picture. The figures are best used to indicate the base levels of the clouds and their compositions. However, cloud base levels can vary considerably from

Figure 2. Thermochemical equilibrium model cloud locations for the jovian planets. Models for Jupiter and Saturn were constructed by S. K. Atreya and M. Wong, based on S. K. Atreya & P. N. Romani (1985). Those for Uranus and Neptune were first published by de Pater, Romani & Atreya (1991).

one location to another depending on the relative humidity at each location. The Galileo Probe Nephelometer instrument (Ragent et al. 1998) detected a cloud base in Jupiter's atmosphere near the 1.34-bar pressure level rather than the predicted location but consistent with knowledge that cloud-forming molecules are significantly subsaturated in the region through which the probe descended (Niemann et al. 1998).

Theoretical models for cloud particle size distributions and microphysical processes are severely impeded by lack of detailed knowledge of atmospheric dynamics and relative humidities of condensable constituents on small scales. Nevertheless Rossow (1978) and Carlson, Rossow & Orton (1988) tried to estimate what to expect from general considerations assuming solar or enhanced abundances of condensible species. Examination of their results is of some inter-

est although the models cannot be expected to reproduce derived particle sizes from observations for Jupiter.

3. Observations of Clouds

3.1. Jovian Hot Spots and 5-μm Opacity

The only *in situ* measurements of clouds obtained thus far were carried out by instruments on the Galileo Probe which descended into an unusually dry region in Jupiter's atmosphere. As mentioned earlier, abundances of volatiles and cloud particles measured by probe experiments are characteristic of a desiccated part of the atmosphere and are unlikely to be representative of Jupiter's average atmosphere. Yet these relatively sparse dry regions allow thermal flux to escape from deeper layers. In the 5-μm window region of the spectrum they dominate Jupiter's emitted flux. Since the 5-μm window contains spectral lines diagnostic of Jupiter's deep water abundance our view of Jupiter's water abundance from remote sensing spectroscopy is biased toward low values. In fact Jupiter's true average deep water abundance is still very much uncertain, although it was trending toward solar composition in the deepest of the probe mass-spectrometer measurements (Niemann et al. 1998). This should serve as a cautionary note to future analyses of spatially unresolved extrasolar planet spectra.

The sparse dry regions which appear bright at 5μm are called hot spots, with the implicit acknowledgment that the terminology refers to appearance, not physical temperature which varies little from one region to the next. Brightness variations at 5μm are very subdued in Saturn's atmosphere, indicating that considerable cloud opacity is ubiquitous on Saturn. Emissions at 5μm are undetectable from Uranus and Neptune because of the colder temperatures and abundant cloud cover for those planets. Images of Jupiter at 5μm show a great deal of structure and temporal variability (Fig. 3). It is difficult to know the altitudes of the clouds responsible for modulating the 5μm emission, but dynamical considerations as well as evidence from images in near-infrared methane absorption bands point to highly variable clouds at the base of the ammonia cloud or deeper.

3.2. Methane Band Images of Jupiter

Observations in methane bands are also diagnostic of cloud opacity and are sensitive to cloud altitude. The two images of Jupiter shown in Fig. 4 illustrate this point. Jupiter's appearance in the continuum window near 0.953μm (4a) is dominated by contrasts which are thought to be produced by absorbing particles and/or weak methane absorption in regions where photons can penetrate to deep levels. Methane is uniformly mixed in Jupiter's atmosphere and so contrasts modulated by methane absorption derive from variations in photon path length in the atmosphere. The composition of the absorbing particles remains unknown, but compounds involving sulfur and possibly nitrogen and carbon are leading candidates.

At a nearby wavelength in a strong methane absorption band (Fig. 4b) contrasts appear which are not seen in the continuum band. These are due to height and scattering opacity variations from cloud particles. Jupiter's Great Red Spot

Figure 3. Jupiter's appearance at 5μm is a pattern of bright hot-spot regions embedded in darker areas whose cloud opacity is sufficient to block most of the upwelling radiation. This image was obtained at the Infrared Telescope Facility (Courtesy G. Orton).

is prominently seen as a region of relatively high, dense clouds. High clouds are also present over the equatorial zone and in the polar regions. The latter are also very dark at UV wavelengths, a signature of high-altitude stratospheric haze probably produce by hydrocarbon chemistry driven by charged particle deposition in auroral regions. Photochemistry is also a driver for stratospheric particle production and is expected to be quite important in extrasolar giant planets close to the primary star or within 30 AU of a hot, luminous star.

Outside the polar regions variations in tropospheric cloud optical depth and altitude are responsible for Jupiter's appearance in strong methane bands. Analyses of limb darkening as well as images and spectra in bands of different strength are used for vertical sounding. Images in weak methane absorptions which probe to several bars pressure in the absence of clouds are not correlated with 5-μm emissions, even though both potentially probe the same vertical region of the atmosphere (West, Kupferman & Hart 1985).

Cloud structure inferred from near-infrared reflected sunlight images is very different that that inferred from 5-μm images. What appear to be deep clear regions in 5-μm regions are not perceptible as low-opacity regions in near-infrared methane images. In order to reconcile these two views West et al. (1985) and West, Strobel & Tomasko (1986) postulated an ubiquitous, optically thick (several optical depths at visible wavelengths) high-troposphere layer of small particles (radius less than one micrometer) in the pressure range 200-500 mb, and clouds of larger particles (3-100 μm radius) near the base of the ammonia cloud region ($\sim$ 600 mb), and in the deeper NH_4SH cloud region and possibly also in the water cloud region. The ubiquitous small particle component is highest and thickest near the equator and accounts for the high reflectivity in the strong methane band near the equator (on Saturn as well). The deeper larger-particle

Figure 4. In the near-infrared Jupiter's appearance is dominated by reflected sunlight. Contrast at 0.953 μm (4a) is governed by some combination of concentrations of absorbing particles of unknown composition and weak methane gas absorption for deeper-penetrating photons. Contrast in a strong methane band at 0.89μm (4b) depends primarily on the density and altitude of scattering particles which limit methane absorption by scattering photons back to space

clouds are responsible for modulating the longer-wavelength (5μm and longer) emissions.

The cloud structure scenario proposed by West et al. (1986) is shown schematically in Fig. 5. Above the ammonia cloud base the static stability of the atmosphere increases due to solar heating. In the statically stable region vapor and small particles carried aloft by slow upwelling in zones (anticyclonic shear zones) or by convective overshooting from small energetic storms can remain for long periods of time, and be transported poleward or equatorward to cover cyclonic bands as well. Larger particles fall out the atmosphere rapidly. Deeper in the atmosphere where convection is vigorous clouds of larger particles form in moist upwelling regions and are diminished or absent from dry downwelling regions. Time scales for formation and dissipation of these clouds can be short.

3.3. Saturn, Uranus and Neptune

Models for cloud structures on Saturn, Uranus and Neptune are dominated by observations in methane bands, although analyses of thermal emissions and radio occultations from the Voyager missions contribute significantly. Methane reflectivity from Saturn is most sensitive to the location of the top of the tropospheric haze layer which is highest in the equatorial zone and shows a pronounced north/south asymmetry at middle latitudes. This asymmetry is induced by seasonal variations in upper troposphere. Seasonal variations in insolation modulate both radiative (i.e. radiative heating of particles and gas) and dynamical

Figure 5. A schematic representation of Jupiter's vertical cloud structure based on inferences from observations at many wavelengths (from West et al. 1986). Hot spot regions have no water cloud and a relatively weak middle cloud, but retain an optically thick (at visible wavelengths) upper tropospheric haze. Schematic representations for other regions are also shown.

(via control of the static stability) factors which contribute to cloud formation. Tomasko et al. (1984) summarize what is known about Saturn's cloud structure.

Jupiter and Saturn form a pair whose reflected sunlight spectra differ substantially from the pair of Uranus and Neptune (Karkoschka 1998). Raman scattering features are strongly developed in the near-UV spectra of Uranus and Neptune because the photon mean free path samples a very large column abundance of molecular hydrogen in those atmospheres. Methane absorptions are much stronger in the Uranus and Neptune spectra both because of the long path length and because methane is enriched in those atmospheres by an order of magnitude compared to Jupiter and Saturn.

De Pater et al. (1991) interpret microwave emission spectra emitted by Uranus and Neptune to favor models with H_2S clouds rather than NH_3 clouds forming near the 3-bar pressure level, although for Neptune they postulate the existence of an ammonia cloud if upwelling is sufficiently vigorous (see Fig. 2 above). Clouds near the 3-bar pressure level are principally responsible for the appearance of Uranus and Neptune although overlying thin methane clouds are visible as bright patches in methane-band images (Smith et al., 1989). More details on clouds structures and particle properties for Uranus can be obtained from West, Baines & Pollack (1991) while for Neptune see Baines et al. (1995).

Acknowledgments. This work was performed by the Jet Propulsion Laboratory, California Institute of Technology under contract with the National Aeronautics and Space Administration

References

Atreya, S. K. & Romani, P. N. 1985, in Planetary Meteorology, ed. G. E. Hunt (Cambridge, England: Cambridge Univ. Press), 17

Baines, K. H., Hammel, H. B., Rages, K. A., Romani, P. N., & Samuelson, R. E. 1995, in Neptune and Triton, ed. D. P. Cruikshank (Tucson: Univ. of Arizona Press), 489

Carlson, B. E., Rossow, W. B., & Orton, G. S. 1988, J. Atmos. Sci., 45, 2066

de Pater, I., Romani, P. N., & Atreya, S. K. 1991, Icarus, 91, 220

Gierasch, P. J., & Conrath, B. 1993, J. Geophys. Res., 98, 5459

Karkoschka, E 1998, Icarus, 133, 134

Lewis, J. S. 1969, Icarus, 10, 365

Niemann, H. B., Atreya, S. K., Carignan, G. R., Donahue, T. M., Haberman, J. A., Harpold, D. N., Hartle, R. E., Hunten, D. M., Kasprzak, W. T., Mahaffy, P. R., Owen, T. C. & Way, S. H. 1998, J. Geophys. Res. 22,831

Ragent, B., Colburn, D. S., Rages, K. A., Knight, T. C. D., Avrin, P., Orton, G. S., Yanamandra-Fisher, P. A., & Grams, G. W. 1998, J. Geophys. Res., 103, 22891

Rossow, W. B. 1978, Icarus, 36, 1

Smith, B. A. et al. 1989, Science, 246, 1422

Tomasko, M. G., West, R. A., Orton, G. S., & Tejfel, V. G. 1984, in Saturn, eds. T. Gehrels and M. S. Matthews (Tucson: Univ. of Arizona Press), 150

Weidenschilling, S. J. & Lewis, J. S. 1973 Icarus, 20, 465

West, R. A., Baines, K. H., & Pollack, J. B. 1991, in Uranus, eds. J. T. Bergstralh, E. D. Miner & M. S. Matthews (Tucson: Univ. of Arizona Press), 296

West, R. A., Kupferman, P. N., & Hart, H. 1985, Icarus, 61, 311

West, R. A., Strobel, D. F., & Tomasko, M. G. 1986, Icarus, 65, 161

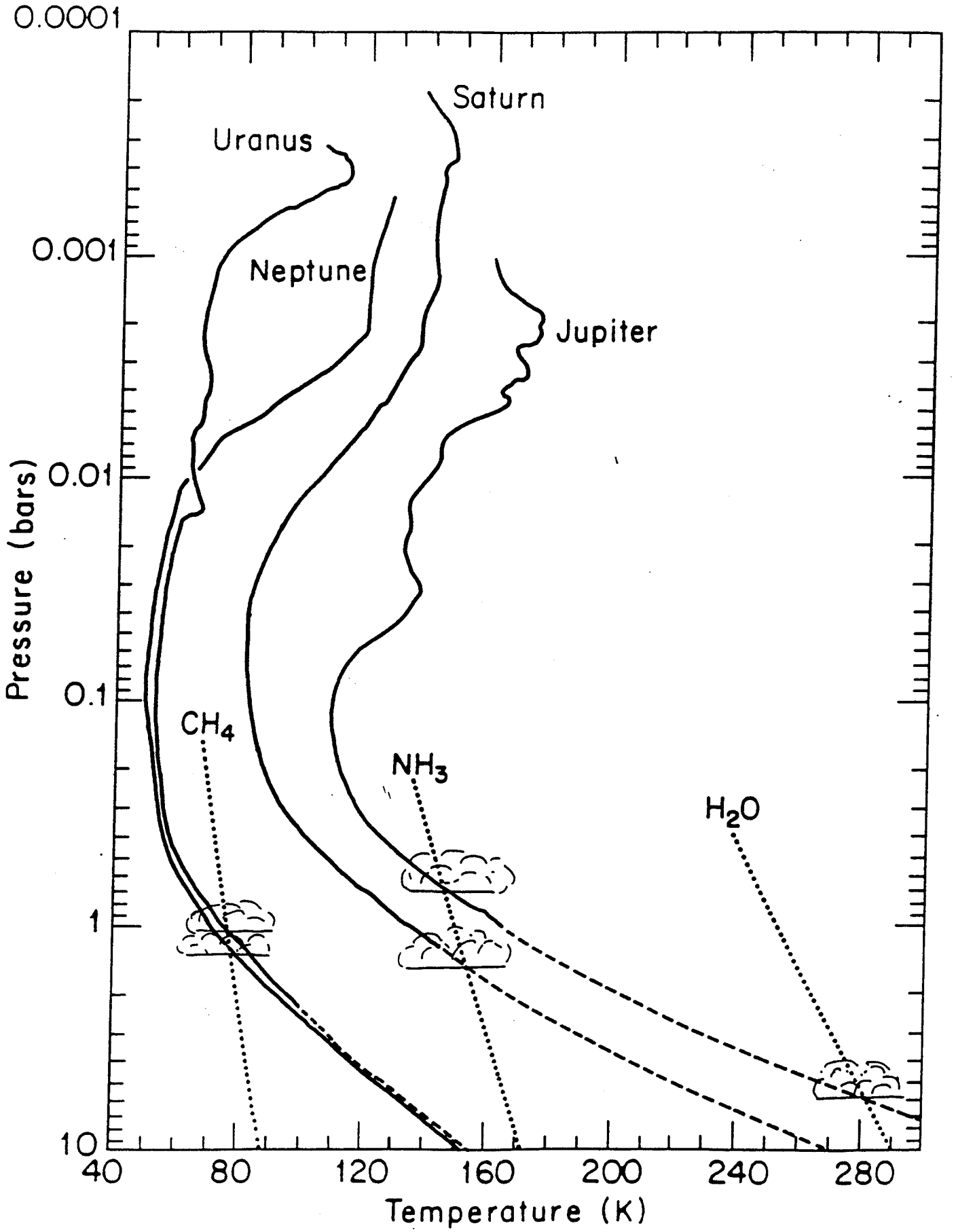
0.0001
0.001
0.01
0.1
1
10
Pressure (bars)
Saturn
Uranus
Neptune
Jupiter
CH_4
NH_3
H_2O
40
80
120
160
200
240
280
Temperature (K)

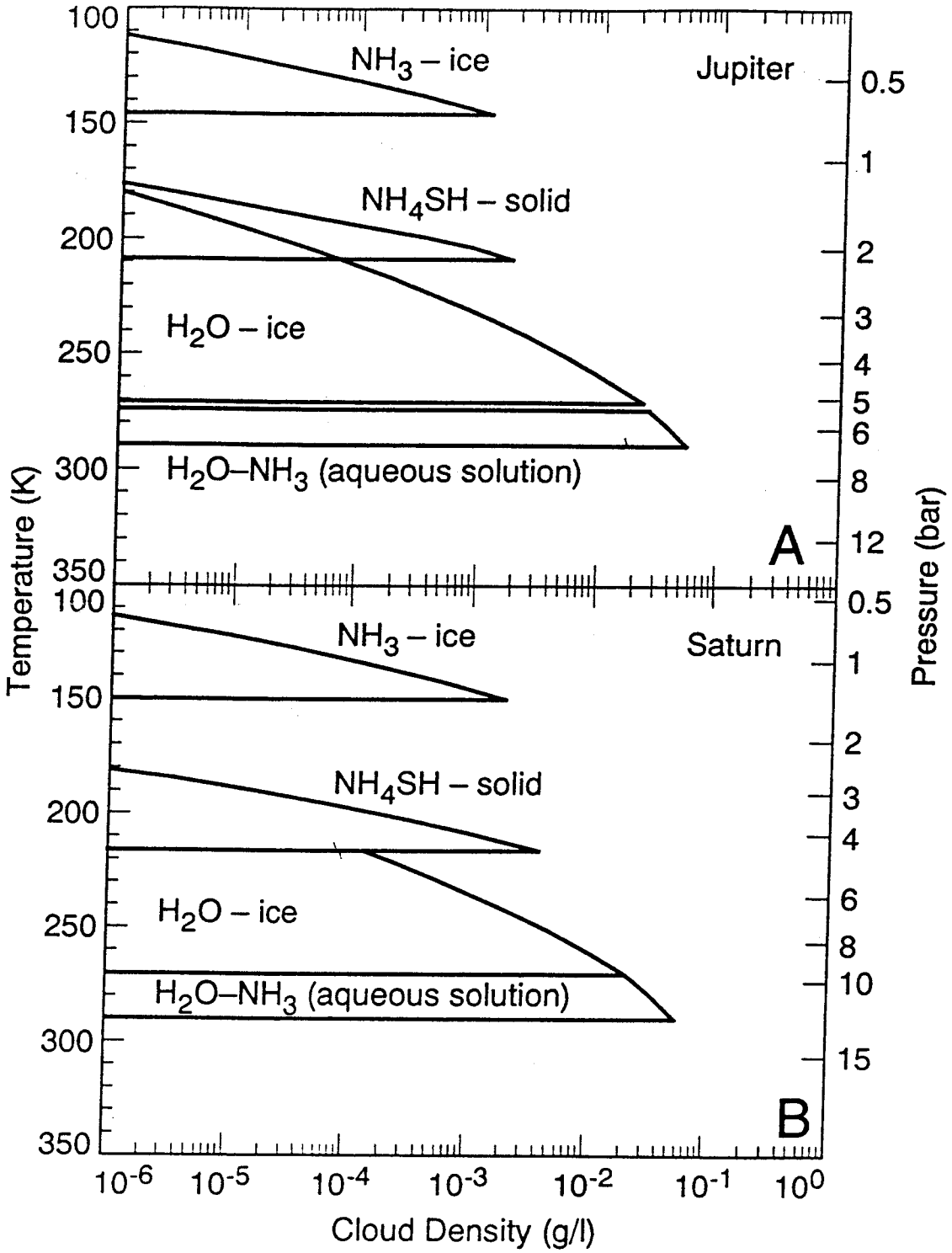
100
150
200
250
300
350
Temperature (K)
NH_3 – ice
Jupiter
NH_4SH – solid
H_2O – ice
H_2O–NH_3 (aqueous solution)
A
0.5
1
2
3
4
5
6
8
12
Pressure (bar)
NH_3 – ice
Saturn
NH_4SH – solid
H_2O – ice
H_2O–NH_3 (aqueous solution)
B
0.5
1
2
3
4
6
8
10
15
10^{-6}
10^{-5}
10^{-4}
10^{-3}
10^{-2}
10^{-1}
10^{0}
Cloud Density (g/l)

2 a b

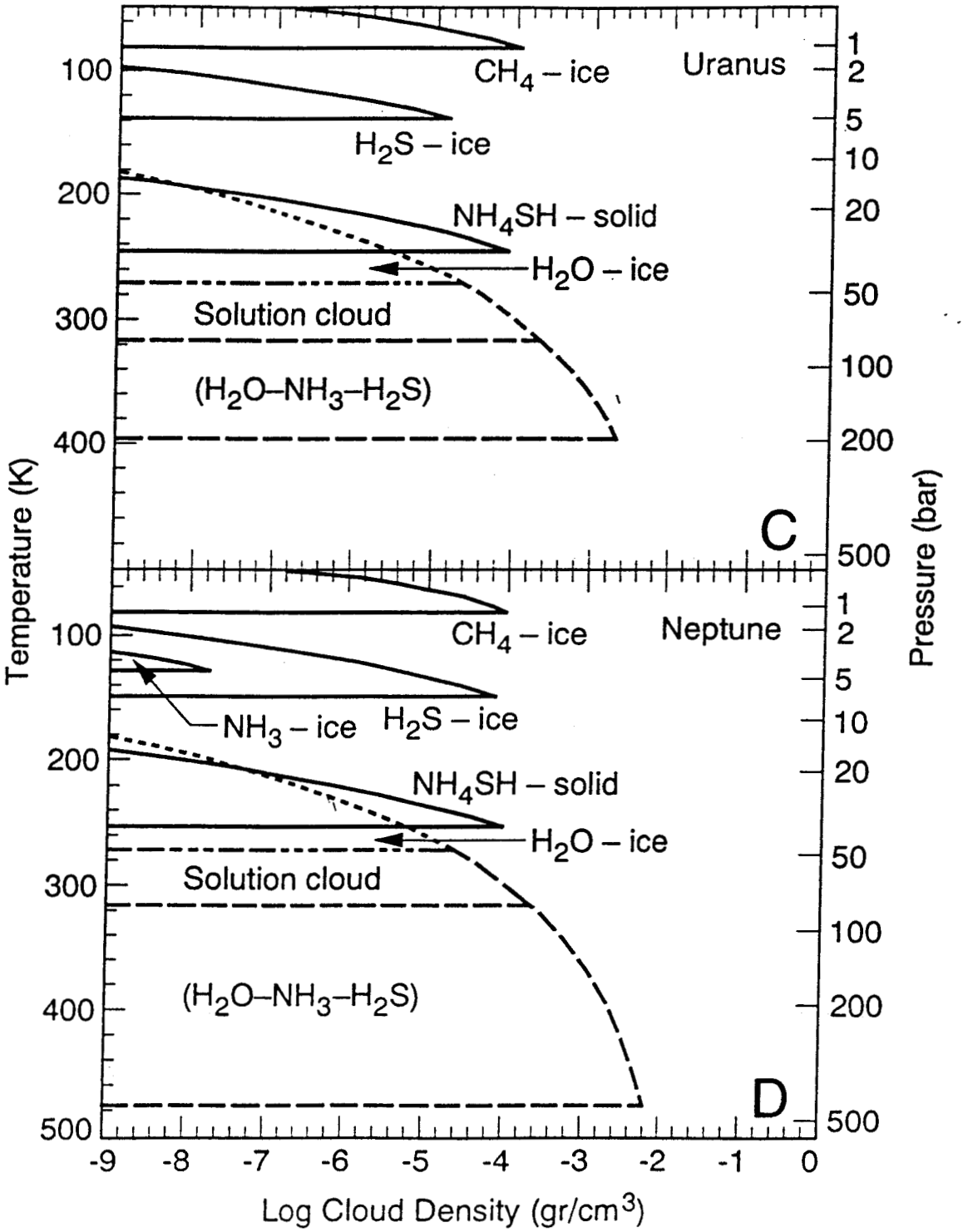
Uranus
CH_4 – ice
H_2S – ice
NH_4SH – solid
H_2O – ice
Solution cloud
(H_2O–NH_3–H_2S)
C
Neptune
CH_4 – ice
NH_3 – ice
H_2S – ice
NH_4SH – solid
H_2O – ice
Solution cloud
(H_2O–NH_3–H_2S)
D
Temperature (K)
100
200
300
400
500
Pressure (bar)
1
2
5
10
20
50
100
200
500
-9
-8
-7
-6
-5
-4
-3
-2
-1
0
Log Cloud Density (gr/cm^3)

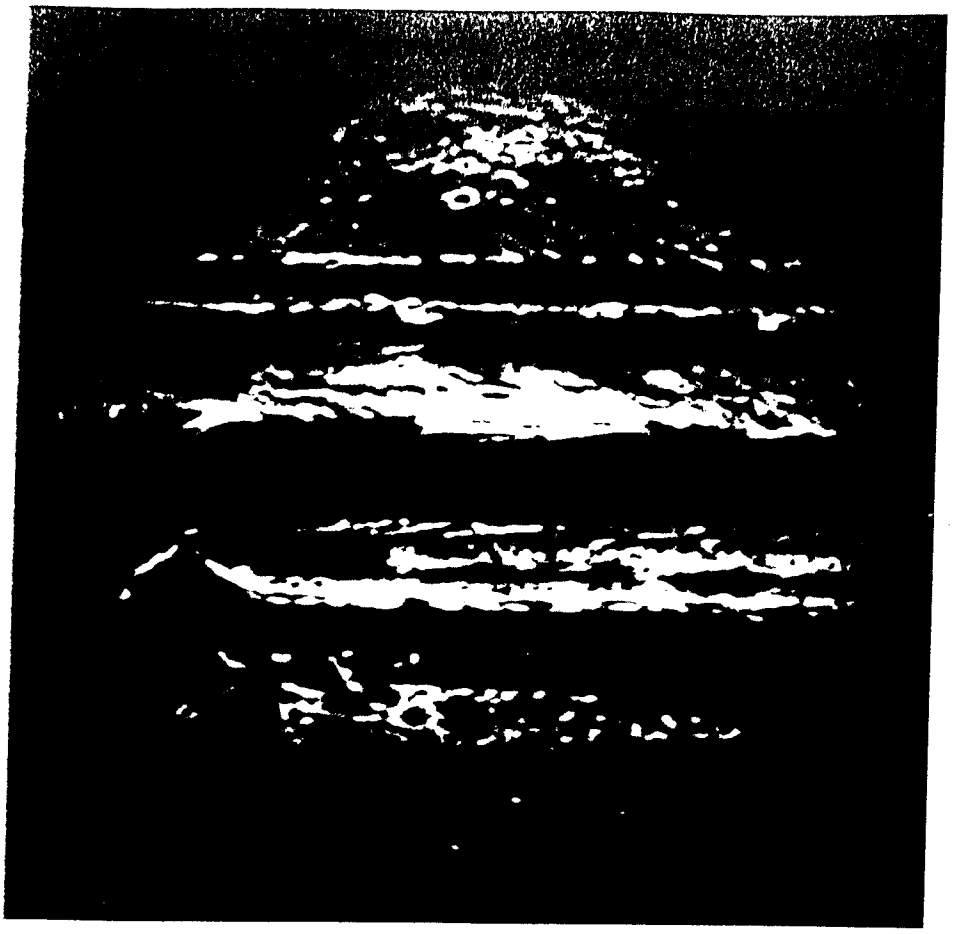

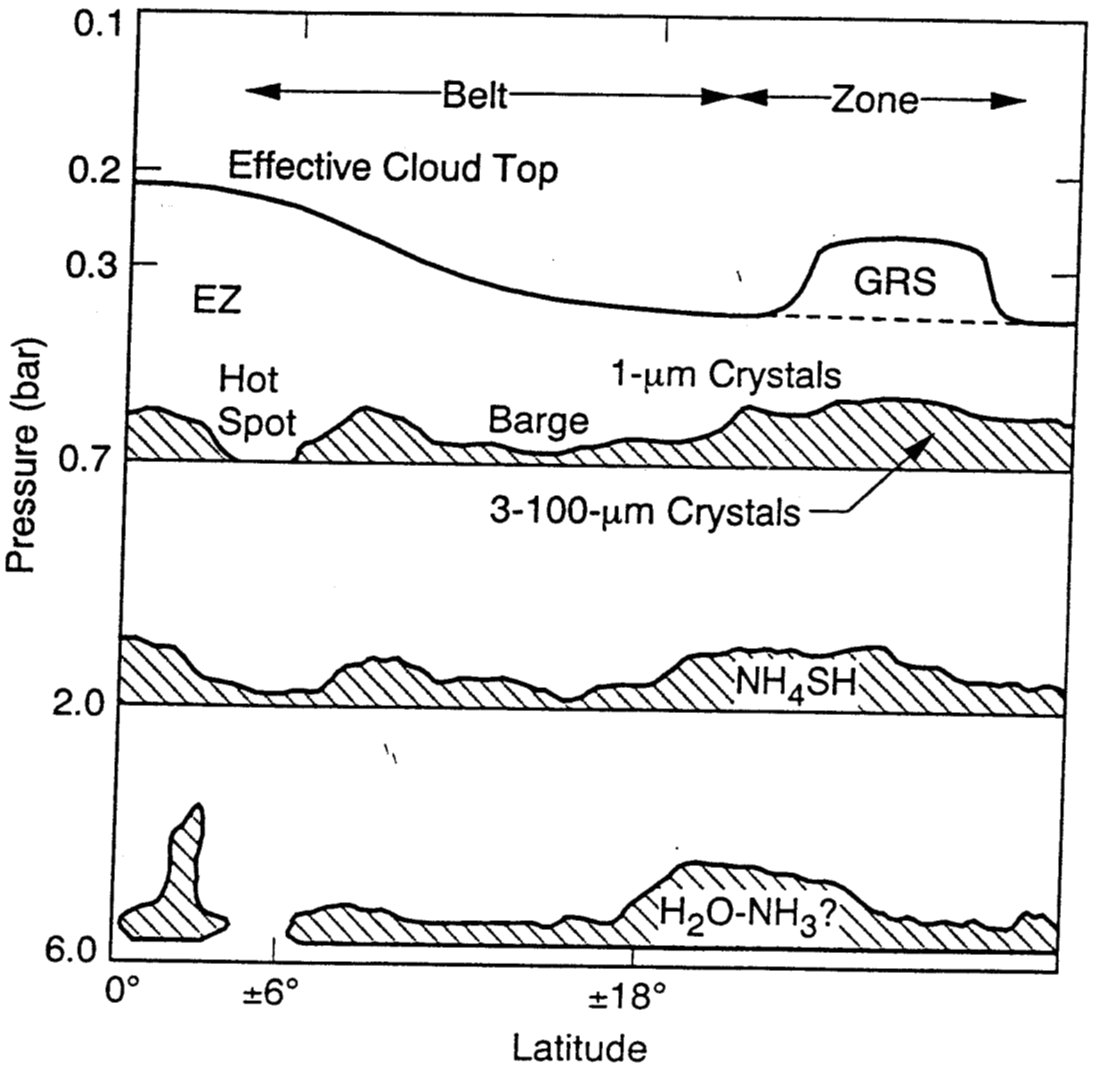
0.1
0.2
0.3
0.7
2.0
6.0
Pressure (bar)
Belt
Zone
Effective Cloud Top
EZ
GRS
Hot
Spot
Barge
1-μm Crystals
3-100-μm Crystals
NH4SH
H2O-NH3?
0°
±6°
±18°
Latitude